

Cross Section for the $(n,2n)$ Reaction in Be^9 †

GEORGE J. FISCHER*
 State University of Iowa, Iowa City, Iowa
 (Received March 14, 1957)

The cross section for the $(n,2n)$ reaction in Be^9 has been measured for neutron energies between 2.6 and 3.25 Mev. It was found that the reaction sets in sharply at approximately 2.7 Mev, from which energy the cross section rises rapidly to 0.70 barn at 3.25 Mev. This experimental result strongly suggests that the reaction proceeds primarily by means of an inelastic interaction which leaves the excited Be^9 nucleus in its 2.43-Mev level before emission of the second neutron upon breakup. There is no peak in the $(n,2n)$ cross section corresponding to the broad peak at 2.73 Mev in the total neutron cross section.

I. INTRODUCTION

A NUMBER of studies of the $(n,2n)$ reaction in Be^9 have been made previously.¹ These measurements, usually made with radioactive neutron sources, indicated cross-section values for the wide energy distributions of these sources of between one-tenth and several barns. Agreement between authors using the same source was often unsatisfactory.

In the present experiment the cross section for this reaction was examined with reasonably monoenergetic neutrons of energies between 2.6 and 3.25 Mev. The choice of this energy region made possible examination of the relation between $\sigma(n,2n)$ and the broad peak in the total neutron cross section which has its maximum at 2.73 Mev. It also made possible an examination of the hypothesis of Fowler, Hanna, and Owen¹ that the $(n,2n)$ reaction proceeds by an inelastic interaction which leaves the excited Be^9 nucleus in the 2.43-Mev level before the second neutron is emitted upon breakup (Fig. 1). The laboratory-system threshold for this mechanism is 2.70 Mev.

II. APPARATUS AND PROCEDURE

A diagram of the experimental arrangement is shown in Fig. 2. A beam of 350-kev deuterons bombarding a "thick" deuterized target at the SUI Cockcroft-Walton accelerator provided energetic neutrons by means of

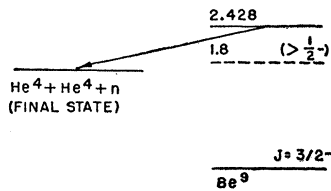


FIG. 1. Portion of energy level diagram of Be^9 .

† This work supported in part by the U. S. Atomic Energy Commission.

* Present address: Argonne National Laboratory, Lemont, Illinois.

¹ A report by H. Agnew [Los Alamos Scientific Laboratory Report LA-1317 (unpublished)] contains many references to earlier work. See also Fowler, Hanna, and Owen, *Phys. Rev.* **98**, 249(A) (1955).

the $\text{D}(d,n)\text{He}^3$ reaction.² Four collimating ports, 2.18 cm in diameter by 56 cm long, were built into the shield at 0° , 54° , 74° , and 88° so that the corresponding median neutron energies emerging from these ports were, respectively, 3.19, 2.92, 2.96, and 2.57 Mev for the stated bombarding energy. The calculated neutron energy distributions for these ports is shown in Fig. 3. The beam emerging from that port which was in use passed through the axis of the beam tube of the activation chamber. The activation chamber contained 125 liters of concentrated potassium permanganate solution during each irradiation. The neutron-detection procedure was a form of the manganese bath technique for counting neutrons.³ Neutrons which emerged from the

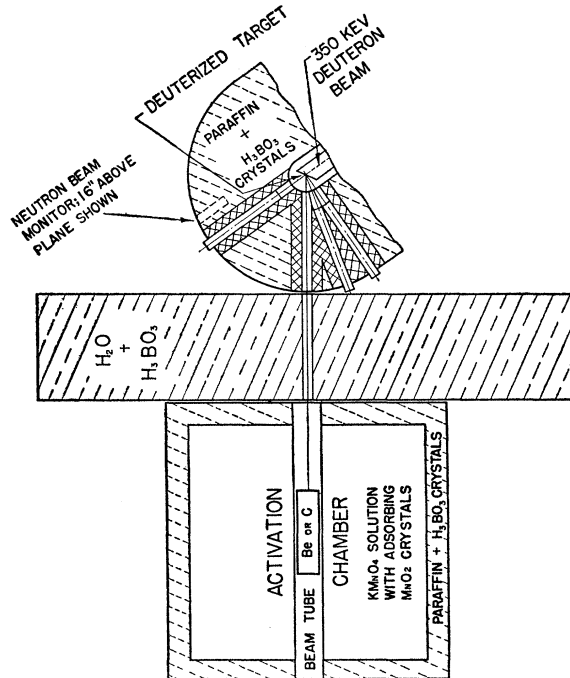


FIG. 2. Diagram of apparatus at accelerator. View is from above.

² Hanson, Taschek, and Williams, *Revs. Modern Phys.* **21**, 635 (1949).

³ *Miscellaneous Physical and Chemical Techniques of the Los Alamos Project*, edited by A. Graves and D. Froman (McGraw-Hill Book Company, Inc., New York, 1952).

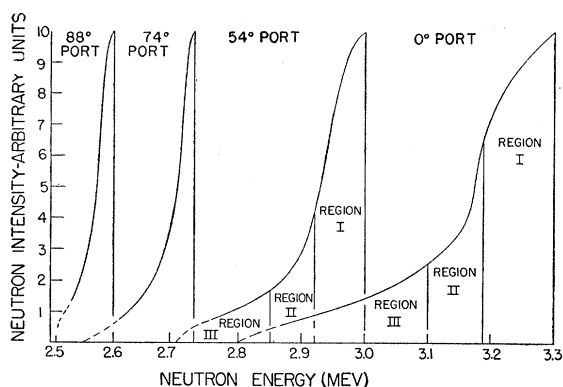


FIG. 3. Neutron energy distributions from beam ports.

neutron target set in the center of the activation chamber would activate manganese atoms and these activated atoms were separated and counted in a manner to be discussed below. The Mn activation was measured in terms of the integrated neutron flux for each irradiation, corrected for decay of the Mn activity to the end of the irradiation.

Irradiations of three separate, identical solutions of potassium permanganate would be made in the course of each determination of $\sigma(n,2n)$. One irradiation was performed with no neutron target in the beam tube in order to determine the "background" activity produced by neutrons leaking in from the room. A second irradiation was made using a carbon target which was essentially opaque to the neutron beam. This target served to scatter the entire neutron beam into the activation chamber. It gave a measure of the activation to be expected if the entire neutron beam underwent only pure scattering events. The third activation was performed with a beryllium target which also was essentially opaque to the incident neutron beam. The magnitude of $\sigma(n,2n)$ was determined by comparing the net activation produced by these two targets using the procedure described in Sec. IV.

Because the beryllium target was rather large (5 cm in diameter and 29 cm long) it was important that the significance of possible multiple collisions within this target upon the resultant activity be examined. A procedure was developed which accounted for these events and at the same time for the dispersion in energy of the incident beam (Fig. 3). The multiple-collision correction amounts to approximately 15% of the result calculated by assuming only a single interaction.

Advantages of the form of Mn bath procedure used here are the complete insensitivity of the detector to γ radiation from any inelastic neutron scattering or capture, the counting efficiency, and the simplicity of the apparatus.

The reliability of the manganese bath procedure was demonstrated by the consistency of results obtained using a Ra-Be neutron source in the center of the

activation chamber. Irradiations made with this source for the same length of time were identical within the 1% counting statistics of the measurements. The activations were also insensitive to variations in amount of MnO_2 crystals added or degree of stirring.

The neutron beam was continuously monitored by means of a BF_3 proportional counter set in the collimating shield. The efficiency of this counter was checked before and after each irradiation by means of a Ra-Be source set in fixed geometry near the counter. The alignment of the beam spot on the rotating target with respect to the axes of the collimator and activation chamber was carefully checked before each of the three irradiations involved in each determination of $\sigma(n,2n)$.

It is felt that the principal experimental uncertainty is a result of instability of the ion source under the relatively high beam currents used for these measurements. This instability made possible changes in the room background to which the activation chamber was somewhat sensitive. Further, because of an undetected error in one of the beam-defining slits, it was possible for the beam spot to migrate a distance of about 2 mm from its desired limits, reducing the effectiveness of the design of the neutron collimating optics of the system. The consequences of these uncertainties are perhaps best estimated by examining the differences between the separate measurements made at each energy port. To some degree the numbers reported here should be taken as an upper limit to the $(n,2n)$ reaction cross section.

III. PROCEDURE FOR DETECTING NEUTRONS

The procedure for detecting neutrons might be described as a form of Szilard-Chalmers reaction. Neutrons which enter the potassium permanganate solution of the activation chamber are slowed down in the aqueous solution. Approximately 14% of the neutrons are captured by the Mn atoms of the 0.22 molar (almost saturated) solution while most of the remaining neutrons are captured by hydrogen of the water. (Mn has a 13.2-barn thermal-neutron capture cross section and a 2.59-hour half-life for decay by β emission.⁴) Upon capturing a neutron, the activated Mn atom emits a γ ray and recoils with sufficient momentum to separate from the permanganate ion. This atom, in its strongly oxidizing environment, is converted to an insoluble MnO_2 molecule. Inactive MnO_2 crystals, grown to sufficient size to be easily separable from the solutions by relatively coarse sintered-glass filter funnels, were added to the potassium permanganate solution before each irradiation was begun and the solution was stirred vigorously during each irradiation. The activated molecules became

⁴D. J. Hughes and J. A. Harvey, *Neutron Cross-Sections*, Brookhaven National Laboratory Report BNL-325 (Superintendent of Documents, U. S. Government Printing Office, Washington, D. C., 1955).

adsorbed on the surface of the large, inactive crystals. After an irradiation of approximately $2\frac{1}{2}$ hours the entire solution was removed from the activation chamber and run through medium-coarseness sintered-glass filter funnels. The carrier crystals with their adsorbed activated molecules were carefully transferred from the filter disks to a small, flat cup which was then set in a fixed geometry between $\text{NaI}(\text{Tl})$ crystals on two photomultiplier tubes. The γ activity following β decay of the Mn was counted for 4000 seconds to give $\frac{1}{2}\%$ counting statistics. The discriminator cutoff was set in the valley below the total absorption peak of the prominent 0.845-Mev γ ray which occurs in this decay.⁵ Two separate determinations of $\sigma(n, 2n)$ were made at each neutron beam port.

IV. ANALYSIS OF DATA

A. Single-Interaction Case

The estimation of the cross section for the $(n, 2n)$ reaction in Be^9 was performed by comparing the activity produced by an essentially opaque carbon target to that produced when an equally opaque target of beryllium was used in the beam tube of the activation chamber. Since neutron reactions with carbon in which the neutron disappears are negligible for the neutron energies of this experiment,⁶ it was assumed that the elastic scattering cross section of carbon was equal to its total neutron cross section. The total cross section of Be^9 was considered to consist of elastic scattering, the (n, α) reaction,⁷ and the $(n, 2n)$ reaction. Several experiments⁸ indicate that σ_γ is negligible for the neutron energies employed here. Thus, the total neutron cross section of beryllium may be written as

$$\sigma_t = \sigma_{sc} + \sigma(n, \alpha) + \sigma(n, 2n).$$

The further assumption, that each neutron makes only one interaction within the Be target, will be made here and removed later in this section.

TABLE I. Experimental results and $\sigma(n, 2n)$ values.

Neut. beam port	\bar{E}_n	$\left(\frac{I(\text{Be})}{I(\text{C})}\right)_{\text{expt.}}$	$\text{Av.}\left(\frac{I(\text{Be})}{I(\text{C})}\right)_{\text{expt.}}$	Single-int. $\sigma(n, 2n)$ barns	Multi-coll. $\sigma(n, 2n)$ barns
0°	3.19	1.246, 1.238	1.242	0.678	0.650
54°	2.93	1.049, 1.092	1.070	0.372	0.310
74°	2.69	0.9634, 0.9972	0.9803	0.030	No calc
88°	2.57	0.9825, 0.9616	0.9726	0.016	No calc

⁵ F. R. Metzger and W. B. Todd, Phys. Rev. **96**, 904 (1953).
⁶ F. Ajzenberg and T. Lauritsen, Revs. Modern Phys. **27**, 77 (1955).

⁷ E. C. Campbell and P. H. Stelson, Bull. Am. Phys. Soc. Ser. II, **2**, 29 (1957); P. H. Stelson and E. C. Campbell, Phys. Rev. **106**, 1252 (1957). The author is grateful to Dr. Campbell and Dr. Stelson for a preprint of their work.

⁸ Scherrer, Allison, and Faust, Phys. Rev. **96**, 386 (1954); Grace, Beghian, Preston, and Halban, Phys. Rev. **82**, 969 (1951).

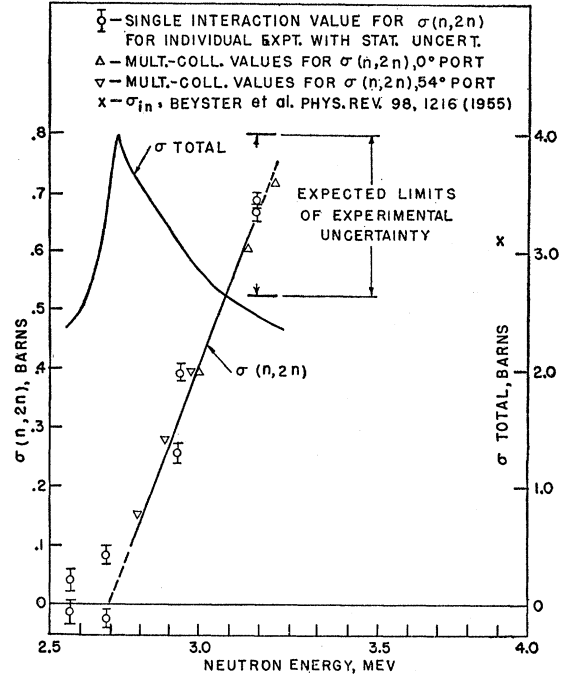


FIG. 4. Cross section for $(n, 2n)$ reaction in Be^9 vs neutron energy.

If the total neutron cross section of Be^9 were entirely an elastic scattering cross section, then the ratio $I(\text{Be})/I(\text{C})$ of the activity produced when the Be target was in the neutron beam to that produced when the C target was in the neutron beam, for normalized experimental conditions, would be exactly equal to one. If σ_t of Be^9 were equal to $\sigma(n, \alpha)$, then, under the same conditions, $I(\text{Be})/I(\text{C})$ would equal zero, while if σ_t of Be^9 were equal to $\sigma(n, 2n)$, then $I(\text{Be})/I(\text{C})$ would equal two. For the general case,

$$I(\text{Be})/I(\text{C}) = \sigma_{sc}/\sigma_t + 2\sigma(n, 2n)/\sigma_t + 0\sigma(n, \alpha)/\sigma_t,$$

from which

$$\sigma(n, 2n) = [I(\text{Be})/I(\text{C}) - 1]\sigma_t + \sigma(n, \alpha).$$

For this calculation all neutrons of each beam port were assigned a single energy, the median neutron energy for that port. The experimental values of $I(\text{Be})/I(\text{C})$ found for each port and the values of $\sigma(n, 2n)$ obtained by use of the above equations are given in Table I. Figure 4 shows these results in graphical form.

B. Treatment of Multiple Collisions

Because the beryllium target was of considerable size, as mentioned earlier, there was a significant probability that a neutron which had been elastically scattered on its first interaction in the Be target would interact one or more times again before emerging from the target, possibly undergoing an $(n, 2n)$ reaction, which would tend to increase the net activation, or an (n, α) reaction, which would tend to reduce the net

activation. Thus, it was important that a multiple-collision procedure be developed which could account for these events. Because it happened, however, that the $(n,2n)$ reaction cross section decreased rapidly with energy, neutrons which were scattered once, and thereby moderated, had considerably reduced probabilities of producing $(n,2n)$ reactions on succeeding interactions. This fact and the small value of $\sigma(n,\alpha)$ at all energies made the total effect of the multiple-collision analysis quite small. Since this analysis provides a correction of less than 15% on the single interaction result, the procedure for treatment of multiple collisions within the Be target will only be outlined in this paper. Details of the procedure are contained in the thesis from which this report is taken.⁹

It should be noted that since carbon is considered here to be a pure elastic scatterer and the activation chamber is essentially a 4π detector, nothing is gained by making a multiple-collision analysis for the carbon target.

From the values for $\sigma(n,2n)$ estimated using the single-interaction calculation, an estimate was made of the probable values of $\sigma(n,2n)$ which would result from taking account of second- and third-order interactions. It was assumed that the corrected curve would deviate from the single-interaction curve by some fractional amount. By the procedure to be outlined, the value of $I(\text{Be})/I(\text{C})$ which would result from the use of the estimated $\sigma(n,2n)$ values was calculated and compared to the experimental results. This led to a revised estimate of $\sigma(n,2n)$ and a new calculation of $I(\text{Be})/I(\text{C})$. It was possible to find a set of values of $\sigma(n,2n)$ which agreed with the experimental value after one or two interactions of this procedure. Since the single-interaction calculations indicated an essentially zero $(n,2n)$ cross section for the two lower energy ports, this method was not applied to these two cases. The effect would have been to raise the value of $\sigma(n,2n)$ slightly (by an amount within the statistical error) by accounting for the net activation loss resulting from later collisions because the (n,α) cross section is larger in these regions than the $(n,2n)$ cross section.

The neutron beam incident upon the target was divided into energy groups indicated by regions I, II, and III in Fig. 3. All neutrons in each of these groups were assigned the single median energy of that group. The various reaction probabilities upon the first interaction were calculated by using cross-section values appropriate to each group. Neutrons which underwent (n,α) reactions contributed nothing to the Mn activation. For each (endothermic) $(n,2n)$ reaction two low-energy neutrons were assumed to enter the activation chamber, while each scattered neutron either entered the activation chamber or became the

source of second- or third-order interactions. The singly scattered neutrons were assumed to remain in their previous energy group or enter lower energy groups according to probabilities calculated using the differential scattering data of Meier and Ricamo.¹⁰ Each scattered-neutron group was assigned a weighted path for emergence from the target.

The effect of second interactions at the new energies was calculated as for the first interaction except that simple escape into the activation chamber was now another possibility. Since many neutrons have escaped from the target after the first and second interaction and since the probability of an $(n,2n)$ reaction is considerably reduced for the energy-degraded twice-scattered neutrons (Fig. 4), the effect of the third interaction is quite small. For this reason the effect of the third interaction was calculated as was that for the second interaction, but with some simplifying assumptions. No higher order interactions were considered.

The results of the multiple-collision analyses for the two higher energy ports are indicated by triangles in Fig. 4. The agreement of the single-interaction and multiple-collision results is largely a fortuitous result of the choice of the single neutron energy for which the single-interaction results at each beam port were calculated. Single-interaction calculations for a beam divided into the three energy intervals of the multiple-collision analysis (Fig. 3) results in an activation ratio $I(\text{Be})/I(\text{C})$ which is approximately 12% too low for the 0° port and 7% too low for the 54° port.

V. CONCLUSIONS

It may be seen from Fig. 4 that there is no peak in $\sigma(n,2n)$ of Be^9 corresponding to the peak in the total neutron cross section of this element. Instead, the $(n,2n)$ cross-section curve rises rapidly above approximately $E_n=2.7$ Mev. The threshold for this reaction is 2.7 Mev if the reaction proceeds by an inelastic interaction which leaves the excited Be^9 nucleus in the prominent 2.43-Mev level before the breakup which yields the second neutron (Fig. 1). Thus, the results of this experiment indicate that this mechanism, which was first suggested by Fowler, Hanna, and Owen,¹ provides the major contribution to the yield of the $(n,2n)$ reaction over the energy region studied.

The results presented here represent the practical limit of the range of neutron energies available from the Cockcroft-Walton accelerator which was used. An extension of these measurements beyond the present range should produce a curve for $\sigma(n,2n)$ which does not exceed the value of σ_{in} measured at $E_n=4.0$ Mev by Beyster *et al.*,¹¹ This point is shown in Fig. 4 of this paper. The straight line through the experimental points in Fig. 4 represents merely a smooth fit to these

⁹ G. Fischer, Ph.D. Dissertation, State University of Iowa (unpublished); available through University Microfilms, Ann Arbor, Michigan.

¹⁰ R. Meier and R. Ricamo, *Helv. Phys. Acta* **26**, 430 (1953).

¹¹ Beyster, Henkel, Nobles, and Kister, *Phys. Rev.* **98**, 1216 (1955).

points. An experimental uncertainty of the magnitude of the differences of the separate measurements at each energy should be added to the statistical uncertainties shown in that figure.

ACKNOWLEDGMENTS

It is a pleasure to acknowledge the support of Professor James A. Jacobs who sponsored the work of

this thesis problem. Professor Edward B. Nelson was most helpful during periods of operation of the Cockcroft-Walton accelerator and made several valuable suggestions. Professor Stanley Bashkin and Professor Richard Carlson as well as Dr. Fred Ribe of the Los Alamos Scientific Laboratory deserve sincere thanks for their helpful discussions and friendly interest in the progress of this experiment.

PHYSICAL REVIEW

VOLUME 108, NUMBER 1

OCTOBER 1, 1957

Nuclear Energy Levels in Mn⁵⁵†

M. MAZARI,* A. SPERDUTO, AND W. W. BUECHNER

Physics Department and Laboratory for Nuclear Science, Massachusetts Institute of Technology, Cambridge, Massachusetts

(Received June 17, 1957)

Inelastically scattered protons from manganese targets bombarded with protons from an electrostatic accelerator have been studied with the high-resolution magnetic spectrograph. Forty-three excited states in Mn⁵⁵ have been established in the region between the ground state and 4.0 Mev. The first five of these levels are at 0.127, 0.983, 1.289, 1.527, and 1.884 Mev.

THIS report describes the results of an investigation of the excited states of the nucleus Mn⁵⁵, carried out through studies of inelastically scattered protons. For this work, thin targets of manganese were prepared by evaporation of high-purity metal from a tungsten boat onto thin Formvar films. These targets were bombarded by the proton beam from the MIT-ONR electrostatic accelerator, and the charged-particle groups resulting from this bombardment were analyzed with the broad-range spectrograph. This equipment and details of the experimental procedure have been described in previous publications.¹⁻³

Natural manganese consists entirely of the mass 55 isotope so that the analysis of the charged-particle groups observed was relatively simple. However, the proton spectrum was sufficiently complex so that measurements at various incident proton energies and at various angles were necessary to study various portions of the spectrum in detail. Observations were made with incident proton energies of 6.51, 6.77, 7.03, and 7.45 Mev and at angles of observation of 50, 90, and 130 degrees. Figure 1 shows a typical spectrum taken at 50 degrees with an incident energy of 7.03 Mev. Groups associated with elastic scattering from the various nuclei present in the target are identified by their chemical symbols. The variation of energy of these groups with angle of observation and incident proton

energy showed that, aside from the protons from elastic scattering from the tungsten, chlorine, sulfur, oxygen, nitrogen, carbon, and hydrogen impurities in the target, all the other peaks in the figure were from manganese. A group from the first excited state of S³² is coincident with group (9) from manganese at this energy and angle. Measurements at other angles and incident energies showed that, aside from group (1) in the figure, associated with an excited state at 0.127 Mev, there were none associated with manganese between the elastically scattered one and the one labeled (2) in the figure, which corresponds to an excited state in Mn⁵⁵ at 0.983

TABLE I. Energy levels of Mn⁵⁵ from the Mn⁵⁶(p, p') reaction.

Level	Excitation energy (Mev)	Level	Excitation energy (Mev)
1	0.127±0.005	23	3.037±0.006
2	0.983±0.005	24	3.081±0.006
3	1.289±0.005	25	3.124±0.006
4	1.527±0.005	26	3.158±0.006
5	1.884±0.005	27	3.195±0.006
6	2.197±0.005	28	3.263±0.006
7	2.252±0.005	29	3.340±0.010
8	2.266±0.006	30	3.351±0.010
9	2.288±0.006	31	3.371±0.010
10	2.311±0.006	32	3.378±0.010
11	2.365±0.006	33	3.424±0.008
12	2.397±0.006	34	3.529±0.008
13	2.426±0.006	35	3.587±0.008
14	2.564±0.006	36	3.607±0.008
15	2.727±0.006	37	3.666±0.008
16	2.751±0.006	38	3.706±0.008
17	2.823±0.006	39	3.755±0.010
18	2.874±0.006	40	3.776±0.010
19	2.953±0.006	41	3.832±0.010
20	2.976±0.006	42	3.862±0.010
21	2.991±0.006	43	3.932±0.010
22	3.005±0.006		

† This work has been supported in part by the joint program of the Office of Naval Research and the U. S. Atomic Energy Commission.

* On leave from the National University of Mexico.

¹ Buechner, Braams, and Spurduto, Phys. Rev. **100**, 1387 (1955).

² Buechner, Mazari, and Spurduto, Phys. Rev. **101**, 188 (1956).

³ C. P. Browne and W. W. Buechner, Rev. Sci. Instr. **27**, 899 (1956).